

Subpicosecond Real-Space Charge Transfer in Type-II GaAs/AlAs Superlattices

J. Feldmann, R. Sattmann, and E. O. Göbel

Fachbereich Physik der Philipps-Universität, Renthof 5, 3550 Marburg, Federal Republic of Germany

J. Kuhl, J. Hebling, K. Ploog, and R. Muralidharan

Max-Planck-Institut für Festkörperforschung, Heisenbergstrasse 1, 7000 Stuttgart 80, Federal Republic of Germany

P. Dawson and C. T. Foxon

Philips Research Laboratories, Redhill, Surrey RH1 5HA, United Kingdom

(Received 12 December 1988)

We have directly measured the real-space transfer times associated with $\Gamma \rightarrow X$ intervalley scattering in type-II GaAs/AlAs superlattices by femtosecond optical pump and probe spectroscopy. We demonstrate that the scattering rate for this unique process connecting electron states in different slabs of the superlattice is related to the spatial overlap of the electronic envelope wave functions in the different satellite minima.

PACS numbers: 78.65.-s, 73.20.Dx, 78.47.+p

Carrier scattering processes are of fundamental importance for the understanding of the electrical and optical properties of semiconductors. The strength of the different scattering processes like carrier-carrier, carrier-phonon, or intervalley scattering depends on the interaction potential (Coulomb, deformation potential, etc.) and on the electronic band structure of the respective material. With the realization of high-quality semiconductor quantum wells and superlattices it has become possible to tailor the electronic band structure of a material system due to the effects of carrier confinement and Brillouin-zone folding. Nevertheless, it turned out that the basic hot-carrier scattering processes, which determine the initial relaxation of photoexcited carriers, are not significantly different in bulk materials and in respective structures with reduced dimensionality.¹⁻³ However, additional carrier scattering processes appear in quantum wells (QW) and superlattices, which are not possible in bulk material, e.g., intersubband scattering^{4,5} and real-space transfer.⁶

In this paper we report the first direct experimental determination of intervalley-scattering rates involving a real-space transfer between different slabs of a superlattice. We demonstrate that the scattering rate is determined by the spatial overlap of the respective electron wave functions of the different spatially separated band minima and consequently can be tailored by the geometrical dimensions of the sample structure.

The experiments are performed on type-II $(\text{GaAs})_m\text{-}(\text{AlAs})_n$ short-period superlattices (SPS) (m, n stand for the number of monolayers with thickness $a_0 = 2.83 \text{ \AA}$ in the slabs of GaAs and AlAs, respectively). According to a simple description neglecting miniband formation⁷ and Brillouin-zone folding⁸ these type-II SPS are characterized by a rapid spatial separation of photoexcited electrons and holes. The lowest confined conduction-band states in the GaAs, which are at the center (Γ) of the Brillouin zone in reciprocal space, are at higher energy

than the lowest confined conduction-band states of the AlAs, which are at the X point of the Brillouin zone, whereas the highest confined valence-band states are at the center of the Brillouin zone for both GaAs and AlAs with the confined GaAs states at the higher energy. Consequently, holes are confined in the GaAs layers whereas thermalized electrons are confined in the AlAs.

We have compared in our experiments two type-II SPS grown by molecular-beam epitaxy with $m=n=9$ (9,9) and $m=11, n=24$ (11,24) (see insets in Fig. 1). These two structures correspond respectively to (i) the case of a SPS with strong coupling between adjacent layers and thus large overlap of the Γ - and X -like

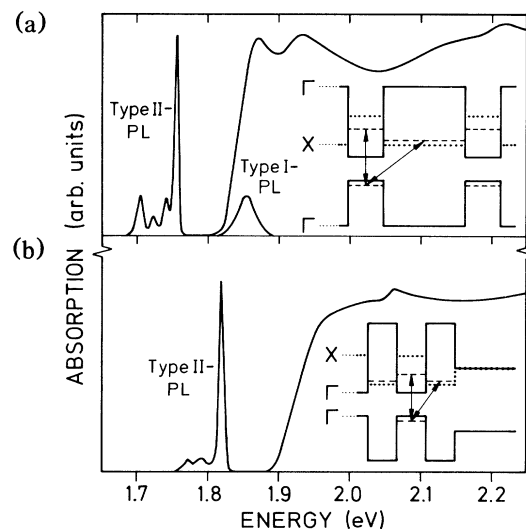


FIG. 1. Absorption spectra of the (a) (11,24) and (b) (9,9) SPS together with the corresponding PL spectra (the luminescence intensities do not have the same scale). Band structures of the samples with the direct type-I and the indirect type-II transitions are schematically shown as insets.

conduction-band states resulting in miniband formation, and (ii) an almost uncoupled SPS with large spatial separation and small overlap of the electron wave functions in the Γ - and X -like states, respectively. In the case of the (9,9) SPS an additional $\text{Al}_{0.4}\text{Ga}_{0.6}\text{As}$ barrier layer is grown on either side of the SPS to prevent diffusion of carriers through the minibands to the substrate or the surface.⁹

The optical properties of these type-II SPS are characterized by weak absorption comparable to indirect-gap semiconductors for transitions involving the spatially separated Γ valence-band states of the GaAs and the folded or unfolded X -like conduction-band states of the AlAs and by strong absorption, typical of a direct-gap semiconductor, at higher energies corresponding to transitions involving the Γ conduction- and valence-band states in the GaAs.¹⁰⁻¹³ The low-temperature transmission (TM) spectra, which basically reflect the absorption, are shown in Fig. 1 for the two samples together with the corresponding photoluminescence (PL) spectra (the substrate of both samples was removed by selective chemical etching). The TM spectra show a sharp increase of the absorption at about 1.85 eV for the (11,24) SPS (upper part in Fig. 1) and at about 1.94 eV for the (9,9) SPS (lower part) which corresponds to direct transitions between Γ valence-band and Γ conduction-band states. The absorption is lower by typically 2 orders of magnitude at energies corresponding to transitions of electrons to the X -like conduction-band states of the AlAs. The TM spectrum of the (11,24) sample reveals clearly resolved the heavy- and light-hole exciton feature. The additional weak structure at about 2.2 eV is attributed to transitions involving the split-off valence band and electrons in the lowest confined states of the Γ conduction band.¹¹ The direct absorption of the (9,9) SPS, which corresponds to the case of strongly coupled wells, shows a rather broad onset, and the splitting of the light- and heavy-hole exciton feature is not observed because of inhomogeneous broadening due to interlayer and intralayer well-width fluctuations. The weak peak at 2.06 eV is related to absorption in the $\text{Al}_{0.4}\text{Ga}_{0.6}\text{As}$ outer confinement layers.

The photoluminescence spectrum of the (11,24) sample exhibits two main peaks. The high-energy emission is unstructured and relatively broad (FWHM=25 meV) and is located energetically in the low-energy tail of the direct (Γ) absorption. This emission is attributed to recombination of excitons involving electrons at the Γ conduction band of the GaAs, which have not yet been scattered to the energetically lower conduction-band states in the AlAs, and holes in the GaAs. The main low-energy PL corresponds to the zero-phonon recombination of excitons involving electrons in the X conduction-band states of the AlAs and holes in the GaAs.¹¹ These X -like conduction-band states of the AlAs are populated by scattering of electrons from Γ states in the GaAs, where they are generated by the opti-

cal absorption. An upper limit of 20 ps for this Γ - X scattering has been determined by time-resolved luminescence.¹³ The aim of this work was to directly determine the time constants of this scattering process, which is unique to type-II SPS and which involves a real-space charge transfer.

The PL spectrum of the (9,9) SPS shows only one main peak corresponding to the low-energy type-II recombination. The relative strength of the type-I recombination involving Γ conduction-band states is appreciably weaker. As will be shown below, this can be partly attributed to the faster Γ - X transfer in the (9,9) sample as compared to the (11,24) SPS.

In order to determine the Γ - X scattering time constants in the type-II SPS we have performed optical pump and probe experiments with 100-fs time resolution at a sample temperature of 5 K. We employ an experimental setup similar to the one described in Ref. 14. Optical pulses of 70 fs (FWHM of the autocorrelation =100 fs) are generated at 622 nm in a colliding-pulse mode-locked (CPM) ring dye laser using the standard four-prism configuration for intracavity dispersion compensation. The CPM output is amplified in a multipass dye flow cell amplifier pumped by a Cu-vapor laser (repetition rate of 7 kHz). The amplified pulses are subsequently chirp compensated (pulse duration after compensation 80 fs) and split into two; one beam is used for excitation of the sample and the other is used to create the probe continuum in an ethylene glycol jet. We observe a pronounced chirp of the continuum of the order of 8 fs/nm for the spectral range from 550 to 730 nm.¹⁵ Behind the sample the transmitted continuum light is dispersed by a grating spectrometer and recorded with an optical multichannel detector for various delays between the pump and probe pulses.

In Fig. 2 we have plotted energy- and time-resolved differential transmission spectra (DTS) ($\Delta T/T_0$) for both samples. The initial injected 2D carrier density is estimated to be of the order of 10^{12} cm^{-2} . In the case of the (11,24) sample (upper part) we found a pronounced bleaching of the light- and heavy-hole exciton feature shortly after excitation, similar to the results obtained at high temperatures by Knox *et al.*¹⁶ for type-I QW. Screening as well as state filling are the origins of this nonlinear optical behavior. However, as will be discussed in more detail below, the bleaching partly recovers within 1 ps in type-II QW and SPS, whereas the recovery times in type-I systems are much longer as reported by Knox *et al.*¹⁶ In addition to the heavy- and light-hole feature, we observe in the DTS a signal at the position of the split-off transition, which corresponds to bleaching of the exciton transition between the split-off valence band and the Γ conduction band.¹¹ It is important to note that the contribution to the bleaching of this transition due to state filling can only originate from electrons, because holes cannot be excited in the split-off band by the pump laser with 2-eV photon energy.

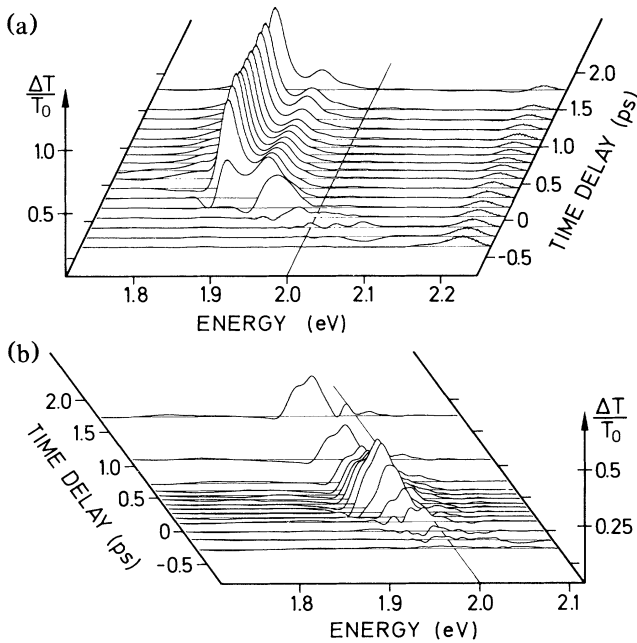


FIG. 2. Energy- and time-resolved differential transmission spectra of (a) the (11,24) and (b) the (9,9) SPS. The pump photon energy is indicated by a line. The representation does not take into account the chirp of the fs continuum. The position $t=0$ refers to the probe photon energy of 2 eV. Since the continuum is positively chirped, the higher-energy position of the continuum is delayed (negative time delay), whereas the low-energy part of the continuum arrives earlier (positive time delay).

The DTS spectra of the (9,9) SPS (lower part in Fig. 2) exhibit only one peak corresponding to bleaching of the direct transition between the Γ valence- and conduction-band states of the GaAs. The weaker structures around the pump-laser energy can be attributed to small fluctuations of the pump-laser spectrum, because a scattered pump-laser signal measured at a large negative delay time is numerically subtracted.

In order to discuss the bleaching and its recovery in more detail, we have plotted in Fig. 3 the differential transmission at energies close to the low-energy onset of the respective excitonic transitions versus time. The unique and important feature of all these traces is the initial subpicosecond partial recovery of the bleaching signal. This initial fast recovery at photon energies close to the low-energy onset of the respective optical transitions is definitely not present in either bulk samples of GaAs or AlGaAs,¹⁷ or in type-I quantum wells.¹⁶ No further appreciable change of the DTS signals apart from the initial partial recovery is observed at these photon energies up to 20 ps. On the other hand, the time-resolved luminescence data prove that the real-space transfer occurs within at most 20 ps.¹³ Altogether, these experimental observations provide convincing evidence to attribute the initial fast recovery to the real-space transfer of

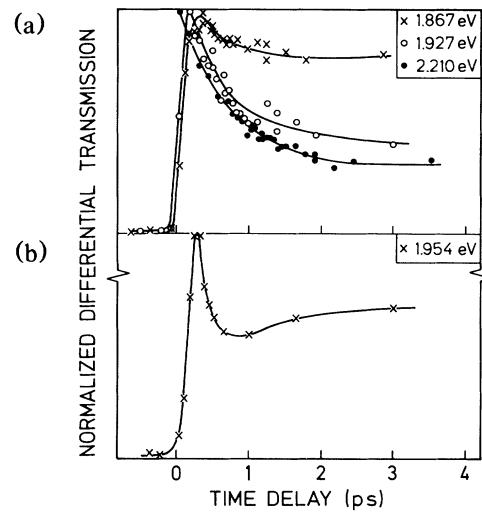


FIG. 3. Time-resolved normalized differential transmission at (a) the hh, lh, and split-off type-I transition energies of the (11,24) SPS and (b) the hh type-I transition energy of the (9,9) SPS. The position $t=0$ for the different curves is corrected for the chirp of the fs continuum. Because of the nonlinearity of the chirp the uncertainty of the $t=0$ position of the trace for 2.21 eV permits a shift of the curve by up to +150 fs.

electrons.

In the lower part of Fig. 3 we have plotted the DTS signal of the (9,9) SPS at an energy of 1.954 eV. We find that initially the bleaching recovers by about 40% with a time constant of the order of 130 fs, which is close to the resolution limit (100 fs) of our present experiment, and subsequently the DTS slowly increases again. The DTS signal is attributed to bleaching of the Γ - Γ transition in the GaAs due to state filling of the states corresponding to the Γ - Γ band edge and screening of the Coulomb interaction. It has been shown previously¹⁸ that state filling is more important in 2D systems. The initial very fast partial recovery reflects the scattering of electrons from the Γ conduction-band states of the GaAs into the X -like states of the AlAs. This electron transfer removes the state filling for the electrons in the Γ valley of the GaAs. In addition, a different contribution to screening may be expected from the scattered electrons since they are confined in the spatially separated AlAs slabs. The remaining signal corresponds to the state filling of the still-occupied hole states of the Γ valence band of the GaAs and possibly to screening of the excitonic enhancement by electrons in the AlAs and holes in the GaAs. Finally, the subsequent slow rise of the DTS signal can be explained by the cooling of the holes. The initial excess energy of the Γ electrons with respect to the X conduction-band minimum heats the hole distribution during the thermalization in the GaAs and the subsequent transfer to the X minimum of the AlAs. Then the carrier system cools again by phonon interaction with the lattice (see also Ref. 13). This results in an increase of

the occupation probability of the states at the band extrema and consequently the bleaching increases again.

In the upper part of Fig. 3 we have plotted the time decays of the DTS signal of the (11,24) SPS for the heavy-hole (hh) and light-hole (lh) exciton peaks as well as for the signal corresponding to the split-off transition. The important results are as follows: The bleaching behavior of the lh and split-off signals are very similar with an initial partial recovery with a time constant of the order of 620 ± 50 fs, respectively. This shows that the initial recovery of the bleaching is due to electron scattering in both cases, because no holes are created in the split-off band. Consequently, the remaining DTS signal in the split-off transition for $t > 1$ ps is purely due to screening of this excitonic transition by electrons in the AlAs and holes in the GaAs. After about 2 to 3 ps the DTS signals become almost constant. The hh signal is qualitatively similar to the DTS curve found for the (9,9) SPS (lower part of Fig. 3); however, the decay constant of the initial partial recovery of the bleaching is much larger. Actually, if we assume that the initial decay is the same for all three signals (hh, lh, split-off) the heavy-hole curve can be fitted qualitatively assuming a rise time for the slow increase of the bleaching due to thermalization of the holes of about 800 fs, which is the same value as obtained from a fit of the (9,9) DTS. We consequently conclude that all three curves have the same time constants for the initial partial recovery of the bleaching. This is in fact expected according to our interpretation attributing the initial fast component to the transfer of electrons from Γ to X conduction-band states in the GaAs and AlAs, respectively. The respective characteristic time constant, however, is appreciably larger for the (11,24) SPS as compared to the (9,9) sample. This difference reflects the different spatial overlap of the electron states at Γ , which are predominantly located in the GaAs, with X -like states, which are predominantly located in the AlAs.

According to simple Kronig-Penney band-structure calculations,¹⁹ we have estimated the probability P_{Γ} of finding an electron with a Γ -like conduction-band state in the AlAs and the probability P_X of finding an electron with a X -like conduction-band state in the GaAs. Whereas P_{Γ} is only slightly higher for the (9,9) SPS (11%) compared to the (11,24) SPS (8%), the values for P_X are higher by an order of magnitude for the (9,9) SPS compared to the (11,24) SPS (19% and 2% for the lowest confined $X_{x,y}$ and 2.5% and 0.1% for the lowest confined X_z states, respectively). This rough estimate already demonstrates that the reduced spatial overlap between Γ and X states in the (11,24) SPS as compared to the (9,9) SPS is responsible for the longer scattering times.

In conclusion, we have determined the time constants for intervalley scattering between conduction-band sub-band states located in different slabs of type-II short-period superlattices. Our results demonstrate that the

time constants associated with this scattering process are determined by the spatial overlap of the wave functions of the different satellite minima involved. This is entirely different from the bulk case, where the interaction potential determines the scattering rate. Finally, we want to stress that the Γ - X scattering in type-II SPS, in spite of the spatial charge transfer involved, can be extremely fast, comparable to, e.g., the Γ - X or Γ - L intervalley scattering in bulk GaAs.^{17,20}

We would like to thank A. Schulz for excellent technical assistance. The work at Marburg is supported by the Deutsche Forschungsgemeinschaft.

¹C. V. Shank, R. L. Fork, R. Yen, J. Shah, B. I. Greene, A. C. Gossard, and C. Weisbuch, *Solid State Commun.* **47**, 981 (1983).

²D. J. Erskine, A. J. Taylor, and C. L. Tang, *Appl. Phys. Lett.* **45**, 54 (1984).

³K. Leo, W. W. Rühle, and K. Ploog, *Phys. Rev. B* **38**, 1947 (1988).

⁴D. Y. Oberli, D. R. Wake, M. V. Klein, J. Klem, T. Henderson, and H. Morkoc, *Phys. Rev. Lett.* **59**, 696 (1987).

⁵A. Seilmeier, H.-J. Hübner, G. Abstreiter, G. Weimann, and W. Schlapp, *Phys. Rev. Lett.* **59**, 1345 (1987).

⁶K. Hess, *Solid-State Electron.* **31**, 319 (1988).

⁷For a first-principles calculation of the band structure in SPS, see e.g., S. Gopalan, N. E. Christensen, and M. Cardona, *Phys. Rev. B* **39**, 5165 (1989).

⁸Because of the Brillouin-zone folding the X minima of the growth direction [001] are folded into the center of the Brillouin zone and hence become quasidirect, whereas the other equivalent X minima remain indirect in k space; see, e.g., M. A. Gell, D. Ninno, M. Jaros, and D. C. Herbert, *Phys. Rev. B* **34**, 2416 (1986).

⁹B. Deveaud, J. Shah, T. C. Damen, B. Kambert, and A. Regreny, *Phys. Rev. Lett.* **58**, 2582 (1987).

¹⁰E. Finkman, M. D. Sturge, M.-H. Meynadier, R. E. Nahory, M. C. Tamargo, D. M. Hwang, and C. C. Chang, *J. Lumin.* **39**, 57 (1987).

¹¹P. Dawson, K. J. Moore, and C. T. Foxon, *Soc. Photo-Opt. Instrum. Eng.* **792**, 208 (1987).

¹²K. J. Moore, G. Duggan, P. Dawson, and C. T. Foxon, *Phys. Rev. B* **38**, 5535 (1988).

¹³G. Peter, E. O. Göbel, W. W. Rühle, J. Nagle, and K. Ploog (to be published).

¹⁴W. H. Knox, M. C. Downer, R. L. Fork, and C. V. Shank, *Opt. Lett.* **9**, 552 (1984).

¹⁵This relatively large chirp may be partly caused by the presence of dispersive optical elements in the probe-beam path; see also, R. L. Fork, C. V. Shank, C. Hirlimann, R. Yen, and W. J. Tomlinson, *Opt. Lett.* **8**, 1 (1983).

¹⁶W. H. Knox, C. Hirlimann, D. A. B. Miller, J. Shah, D. S. Chemla, and C. V. Shank, *Phys. Rev. Lett.* **56**, 1191 (1986).

¹⁷W. Z. Lin, R. W. Schoenlein, J. G. Fujimoto, and E. P. Ippen, *IEEE J. Quantum Electron.* **24**, 267 (1988).

¹⁸S. Schmitt-Rink, D. S. Chemla, and D. A. B. Miller, *Phys. Rev. B* **32**, 6601 (1985).

¹⁹Hung-Sik Cho and P. R. Prucnal, *Phys. Rev. B* **36**, 6 (1987).

²⁰J. Shah, B. Deveaud, T. C. Damen, W. T. Tsang, A. C. Gossard, and P. Lugli, *Phys. Rev. Lett.* **59**, 2222 (1987).